Atmos. Chem. Phys., 16, 12059–12079, 2016
www.atmos-chem-phys.net/16/12059/2016/
doi:10.5194/acp-16-12059-2016

Atmospheric Chemistry and Physics Open Access EGU

Parameterizing cloud condensation nuclei concentrations during HOPE

Luke B. Hande[1], Christa Engler[2], Corinna Hoose[1], and Ina Tegen[2]

[1]Karlsruhe Institute of Technology, Karlsruhe, Germany
[2]Leibniz-Institute for Tropospheric Research, Leipzig, Germany

Correspondence to: Luke B. Hande (luke.hande@kit.edu)

Received: 26 April 2016 – Published in Atmos. Chem. Phys. Discuss.: 4 May 2016
Revised: 9 August 2016 – Accepted: 6 September 2016 – Published: 27 September 2016

Abstract. An aerosol model was used to simulate the generation and transport of aerosols over Germany during the HD(CP)^2 Observational Prototype Experiment (HOPE) field campaign of 2013. The aerosol number concentrations and size distributions were evaluated against observations, which shows satisfactory agreement in the magnitude and temporal variability of the main aerosol contributors to cloud condensation nuclei (CCN) concentrations. From the modelled aerosol number concentrations, number concentrations of CCN were calculated as a function of vertical velocity using a comprehensive aerosol activation scheme which takes into account the influence of aerosol chemical and physical properties on CCN formation. There is a large amount of spatial variability in aerosol concentrations; however the resulting CCN concentrations vary significantly less over the domain. Temporal variability is large in both aerosols and CCN. A parameterization of the CCN number concentrations is developed for use in models. The technique involves defining a number of best fit functions to capture the dependence of CCN on vertical velocity at different pressure levels. In this way, aerosol chemical and physical properties as well as thermodynamic conditions are taken into account in the new CCN parameterization. A comparison between the parameterization and the CCN estimates from the model data shows excellent agreement. This parameterization may be used in other regions and time periods with a similar aerosol load; furthermore, the technique demonstrated here may be employed in regions dominated by different aerosol species.

1 Introduction

The influence that aerosols have on cloud microphysics is relatively well established; however clouds and aerosols continue to contribute the largest uncertainty to the Earth's energy budget in climate simulations (Boucher et al., 2013). In an effort to realistically capture aerosol cloud interactions and hence reduce these uncertainties, cloud condensation nuclei (CCN) parameterizations have been developed for models. The ability of an aerosol to act as a CCN is determined by its size and composition, so accurately modelling CCN activation necessitates an understanding of these underlying physical and chemical properties.

The hygroscopicity parameter is now commonly used to characterize the chemical properties of a given aerosol species (Petters and Kreidenweis, 2007); however for the sake of simplicity, chemical composition can be neglected. Segal and Khain (2006) state that aerosol chemical composition has a relatively small effect and assume all aerosols are composed of NaCl. Some doubt does remain as to the relative importance of the aerosol physical and chemical properties in determining CCN concentrations (Hudson, 2007); however most evidence suggests that number concentration and size have the most significant effect (Dusek et al., 2006; Ervens et al., 2007; Feingold, 2003), since larger particles are more readily activated.

There are numerous possibilities for characterizing the number concentration of aerosols. Early parameterizations, including the seminal work of Twomey (1959), used a power law to describe the number of activated CCN. A power law can also be employed to describe the aerosol population; however this approach combined with simple expressions for

the number of nucleated drops has drawbacks, since anomalously high droplet number concentrations can be produced. A power law is also employed to define the aerosol size distribution (Khvorostyanov and Curry, 1999) in parameterizations of droplet activation (Morrison et al., 2005) employed by the Weather Research and Forecasting (WRF) model.

Other parameterizations assume a prescribed uniform aerosol size distribution with only one typically log-normal mode (Abdul-Razzak et al., 1998; Segal and Khain, 2006). Several modes can be used to define the aerosol sizes (Abdul-Razzak and Ghan, 2000; Fountoukis and Nenes, 2005; Liu et al., 2012; Shipway and Abel, 2010), where the parameters of the size distribution are either calculated from an aerosol model or derived from limited observations from a short time period (Rissler et al., 2004). If coupled to another suitable model, e.g. the CAM-Oslo GCM, the aerosol modes can evolve over time, offering the next degree of complexity. Parameterizations can also employ a sectional representation of the aerosol size distribution (Abdul-Razzak and Ghan, 2002; Nenes and Seinfeld, 2003), which also allows the size distribution to evolve over time.

Perhaps unsurprisingly, a more complex representation of aerosol properties and processes leads to improvements in simulated aerosol forcing (Bellouin et al., 2013; Mann et al., 2012), as well as CCN concentrations (Weisenstein et al., 2007). However these approaches introduce a significant computational burden for simulations, which limits their applicability to short, limited-area simulations.

Segal and Khain (2006) point out that an effective parameterization should be as simple as possible, yet encompass all the governing factors affecting aerosol activation. This sentiment has also been echoed by Petters and Kreidenweis (2007). To this end, we present a parameterization for estimating CCN concentrations which exploits the complexity of an aerosol model to accurately characterize chemical and physical properties of aerosols. All these detailed properties are then represented within a simple mathematical model, which is a function of the vertical velocity and atmospheric pressure. This represents a new approach for parameterizing CCN for use in models. The parameterization is developed for use in the large eddy simulation (LES) version of the ICOsahedral Nonhydrostatic (ICON) model, from modelled aerosol data during the HD(CP)^2 Observational Prototype Experiment (HOPE) campaign. It is suggested the parameterization is suitable for other time periods with a similar aerosol load.

2 Aerosol simulations

The High Definition Clouds and Precipitation for advancing Climate Prediction (HD(CP)^2) project aims at improving our understanding of clouds and precipitation, by building and using a model capable of very high-resolution simulations. An essential component of this project is the use of the ICON model to preform large eddy simulations, as demonstrated by Dipankar et al. (2015). The ICON-LES model has no online aerosol scheme, which motivates the need for the new CCN parameterization developed here. To achieve this, the Consortium for Small-scale Modelling (COSMO) meteorological model coupled to the Multi-Scale Chemistry Aerosol Transport (MUSCAT) (Wolke et al., 2012) model was used to simulate the generation and transport of natural and anthropogenic aerosols to Europe. The time period covers the HD(CP)^2 Observational Prototype Experiment (HOPE) performed in Jülich, Germany, which will provide critical data for model evaluation.

Table 1. Aerosol physical and chemical properties.

Species	κ	σ (µm)	r (µm)	ρ (kg m^{-3})
Amm nitrate	0.54	1.6	0.05	1.725
Amm sulfate	0.51	1.6	0.05	1.77
Dust 1	0.14	2.0	0.2	2.65
Dust 2	0.14	2.0	0.6	2.65
Dust 3	0.14	2.0	1.75	2.65
Dust 4	0.14	2.0	5.25	2.65
Dust 5	0.14	2.0	15.95	2.65
Elemental C	5×10^{-7}	1.8	0.03	1.8
Organic C	0.14	1.8	0.055	1.0
Sea salt 1	1.16	1.8	0.065	2.2
Sea salt 2	1.16	1.7	0.645	2.2
Sulfate	0.236	1.6	0.05	1.8

The aerosol species simulated were ammonium nitrate, ammonium sulfate, dust (5 sizes), elemental carbon, organic carbon, sea salt (2 sizes), and sulfate. Table 1 shows the chemical and physical properties of the simulated aerosols. The hygroscopicity parameter is κ, the mode standard deviation and mean radius are σ and r respectively, and the density is given by ρ. The hygroscopicity parameter for each aerosol species was taken from Ghan et al. (2001).

In COSMO–MUSCAT, the meteorological model COSMO, which is the operational forecast model of the German Weather Service (DWD), is coupled online with the chemistry transport model MUSCAT. Meteorological parameters such as humidity and temperature are interpolated and transferred from COSMO–MUSCAT at each advection time step. This ensures that actual meteorological conditions are represented. MUSCAT computes atmospheric transport and chemical transformations of aerosol species and gas phase reactions. The transport processes include advection, turbulent diffusion, sedimentation, and dry and wet deposition. In addition, size-resolved atmospheric particle number concentrations were simulated for Saharan dust aerosol. While the number distribution of secondary aerosol species are particularly important for determining cloud condensation nuclei concentrations, dust particles are efficient ice nuclei.

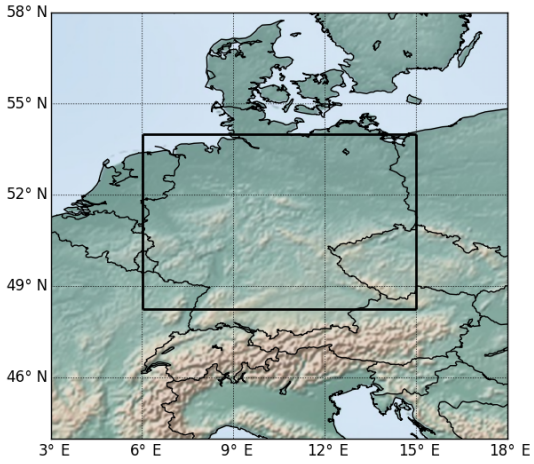

Figure 1. Domain over Germany used in this study.

For the model results shown here, the horizontal grid spacing was 28 km, and 32 vertical layers were used. The domain considered in this study is between 48.25–54° N and 6–15° E, shown in Fig. 1. To ensure that the deviations in the modelled meteorological fields from the real atmosphere remain small, COSMO was reinitialized every 24 h. COSMO ran for 48 h at each cycle, and after 24 h MUSCAT was restarted. Then, both models ran parallel for 24 h at each cycle. For the chemical compounds and aerosol species, MUSCAT computes total mass concentration. The model has been applied and tested for numerous case studies in Germany as well as in annual simulations in the European domain (Wolke et al., 2012).

For the estimation of the aerosol number size distributions, the mode mean diameter, density, and standard deviation of the log-normal mode have been predefined for each aerosol species. Dust size distributions have been described by Heinold et al. (2011). Sea salt modes are determined according to Gong (2003). The simulated mass concentrations were converted to total number concentrations by assuming spherical particles of a certain size and density individually for each component. Assuming a log-normal size distribution with a certain mean diameter and standard deviation, the total number concentration can then be used to estimate the number size distribution for each component. The sum of all individual size distributions results in the total particle size distribution, which can be compared to the observations.

The aerosol mixing state can influence aerosol size distribution and hygroscopicity, hence it influences CCN activity. Wang et al. (2010) shows that mixing state assumption is only important when primary organic aerosol and black carbon dominate aerosol volume. Here, aerosol composition is mostly from ammonium nitrate and ammonium sulfate. Sullivan et al. (2009) show that not all chemical reactions that process atmospheric dust aerosols increase CCN activity. Therefore mixing state assumption should not affect the results strongly. Furthermore, Ervens et al. (2010) show that simple mixing state assumptions are insufficient only very close to the pollution sources.

3 Aerosol measurements and simulation evaluation

Model simulations were performed for the period 26 March to 20 June 2013, which covers the period of the HOPE field campaign in Jülich. Furthermore, the model was evaluated for the site Melpitz near Leipzig (87 m a.s.l.; 51.53° N; 12.90° E) (Engler et al., 2007; Spindler et al., 2013), since no specific aerosol measurements were carried out during the campaign at the Jülich site. Therefore, comparisons of modelled and observed aerosol composition size distributions were performed at the Melpitz site. The station is situated on flat terrain, and no larger sources of pollution lie within close proximity to the station. Particle number size distributions at dry conditions were measured using a twin differential mobility particle sizer (TDMPS) (Birmili et al., 1999, 2016). The major ions and carbon species in the aerosol have been continuously measured from daily filter samples since 2003 (Spindler et al., 2013).

A comparison of modelled and observed chemical species is shown in Fig. 2 for the time period of the HOPE Melpitz campaign. Only the results of modelled and observed concentrations of the species ammonium sulfate and ammonium nitrate as well as the small sea salt mode are shown, as these species dominate CCN concentrations over the model domain. The agreement between the model results and observations of the mass concentrations of secondary aerosol species as well as the sea salt is very good. Both magnitude and temporal variability of the aerosol concentrations are well matched except for the first few days of the time period, where the model underestimates the observed aerosol species, particularly for ammonium nitrate and to a lesser extent for ammonium sulfate and sea salt. Total $PM_{2.5}$, which is computed as the sum of all aerosol types excluding the supermicron size dust and sea salt fractions, is underestimated by the model by about a factor of 2. This underestimate can likely be tied to an underestimated submicron dust emission or secondary organic aerosol (SOA) that is not considered by the model. Zhao et al. (2015) suggest SOAs have hygroscopicity parameters between 0.03 and 0.1, less than the majority of aerosols considered in this study. Therefore, any underestimate in SOA concentration should not affect CCN concentrations significantly.

The modelled aerosol size distribution resulting from conversion of the simulated bulk aerosol concentration into size-resolved aerosol concentration at the Jülich site is shown in Fig. 3 for the example day 18 June 2013 at 12:00 UTC. Here, ammonium sulfate contributes the main part to the modelled aerosol number concentrations. These results could not be verified at the Jülich site due to lack of observations. There-

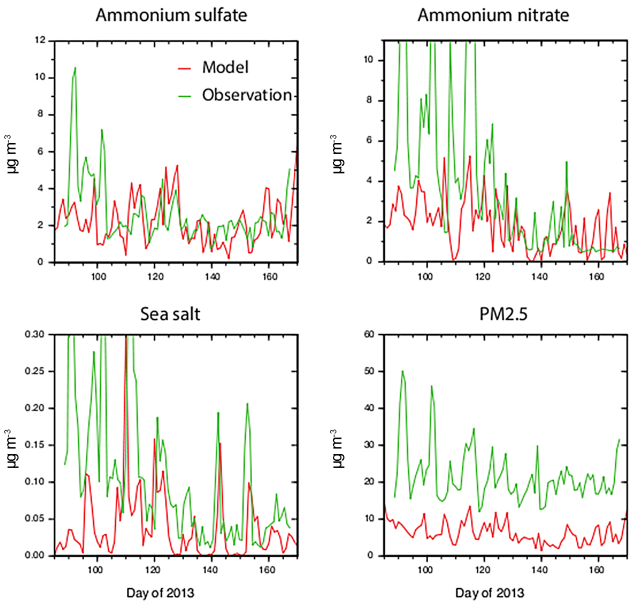

Figure 2. Comparison of the modelled and observed concentrations of aerosol species ammonium sulfate, ammonium nitrate, sea salt, and total $PM_{2.5}$ at the Melpitz site for the HOPE simulation period in spring 2013.

fore, comparisons of modelled and observed size distributions were performed at the Melpitz site (Fig. 3b).

While in the size range between 50 nm and 0.15 µm the model estimated number size distribution matches the observations well, the model underestimates the observations at smaller and larger particle sizes. This is also the case when comparing model results and observations for a full month (Fig. 3c). For particles between about 10 and 30 nm, the model underestimates the number concentration by 1–2 orders of magnitude for the whole month. A smaller discrepancy is seen for course mode aerosols, where the model suggests about half the concentrations given in the observations for 0.5 µm particles. The underestimation at smaller sizes is due to the fact that the nucleation mode, which is present in the measurements, is not taken into account in the model. However, at this size range such an underestimate is less important for diagnosing CCN concentrations. The underestimate of the model results at larger particle sizes (also reflected in underestimates of $PM_{2.5}$ and PM_{10} concentrations, not shown) may be more critical; however the number concentrations of the large particles are low. The model deficit may point to an aerosol type that is not included in the model, for example fugitive dust. Natural sea salt and desert dust aerosol are unlikely to be responsible for this deficit at the larger particle sizes, since the sea salt large mode was adjusted to observations, while independent comparisons of dust aerosol size distributions with observations during measurements at independent field campaigns have shown that simulated dust size distributions in the supermi-

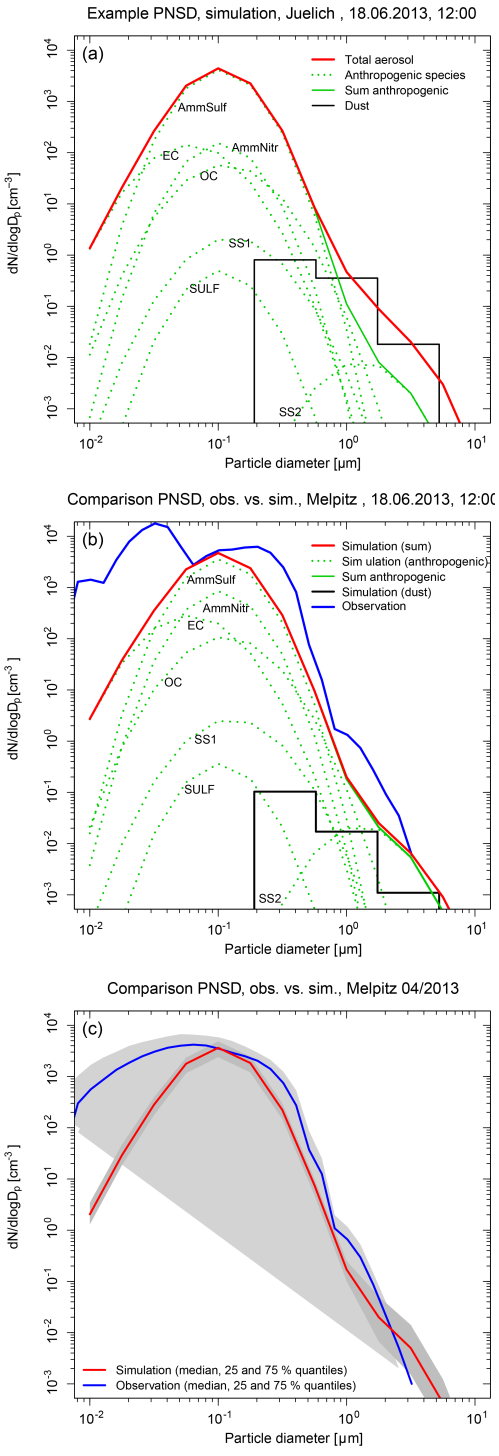

Figure 3. Aerosol particle number size distribution for 18 June 2013 at the sites Jülich **(a)** and Melpitz **(b)**, and for the month April 2013 at Melpitz **(c)**. The red lines mark the resulting simulated aerosol size distributions for the sum of the individual species (dotted green lines). Black lines represent modelled number size distribution of dust transported from the Sahara desert to the sites Jülich and Melpitz respectively.

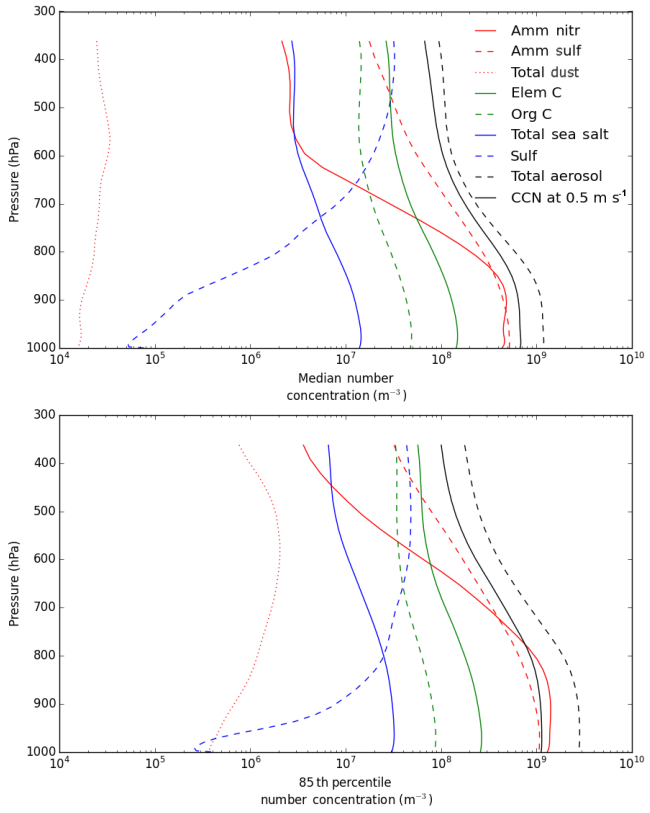

Figure 4. Temporally averaged median (top) and 85th percentile (bottom) number concentration for aerosols and CCN at 0.5 m s^{-1} from 25 March to 16 June 2013.

cron size range match well to ground and airborne dust size observations (Heinold et al., 2011).

4 Aerosol and CCN concentrations during HOPE

Figure 4 shows the temporally averaged median and 85th percentile vertical profiles of the number concentration of all aerosol species and the resulting CCN number concentration at a prescribed vertical velocity of 0.5 m s^{-1}. To calculate the statistics, the domain-wide median and 85th percentile vertical profiles were first calculated at each time step. Then the mean of these profiles was taken over all time steps.

According to Fig. 4, the dominant aerosols in the lower levels are ammonium nitrate and ammonium sulfate, and at higher levels the concentration of sulfate and elemental carbon become more significant. The concentrations of most aerosol species are constant at lower levels, and decrease at higher levels, with the rate of decrease varying between aerosol species. Sulfate is the exception, with concentrations increasing with altitude due to the nucleation of Aitken mode particles in the upper troposphere. In the model, sulfate is formed by the oxidation of SO_2, which instantly reacts to form ammonium sulfate if ammonium is available (Renner and Wolke, 2010). In the upper troposphere, less ammonium is available, which leads to the nucleation of sulfate particles. The median dust concentrations are relatively constant with altitude, as already shown by Hande et al. (2015) during a different time period.

The bottom panel of Fig. 4 shows the temporally averaged 85th percentile concentrations of aerosols and CCN at 0.5 m s^{-1}. Taking the ratio of the 85th percentile concentrations to the median concentrations provides a rough measure of the spatial variability. For example, the 85th percentile for ammonium nitrate is, on average, 5.6 times larger than the median. This increases to 44 times larger for dust, with the smallest difference being 2.1 times for organic carbon. In contrast to this, the 85th percentile for CCN concentrations is only 1.8 times larger than the median concentrations on average. This indicates that, while there may be significant spatial variability in aerosol concentrations, the spatial variability in CCN concentrations is significantly lower.

The spatial variability on shorter timescales, as well as the temporal variability over the course of the HOPE campaign are shown in Fig. 5. The latitudinal and longitudinal median aerosol number concentrations and the resulting CCN number concentrations, averaged over all pressure levels and time steps for 1 day, 30 April 2013, are shown in the top and middle panel, and the bottom panel shows the temporal variability. For this specific day, ammonium nitrate shows a significant amount of variability in both latitude and longitude. Sea salt aerosols also have a large amount of variability with a strong north–south gradient, consistent with the source region being the oceans north of Germany. Indeed, north of the domain, sea salt becomes the dominant aerosol. The important point is that, while there may be large variability in the spatial distribution of aerosols, the spatial variability in the resulting CCN is significantly lower. Even when individual pressure levels are considered, spatial variability in CCN concentrations remains low. The largest variability is in the north–west of the domain above 400 hPa, where concentrations are up to 7 times higher than the rest of the domain. CCN concentrations at 400 hPa are more than 2 orders of magnitude lower than near the surface; therefore the impact of this error is small.

The same conclusion regarding the horizontal homogeneity of CCN number concentrations over Germany can be obtained from analysing other days across the whole campaign time period. The spatial distribution of the aerosols can change significantly, particularly for ammonium nitrate, dust, and sea salt. This is consistent with the findings from analysing the difference between the 85th percentile and the median concentrations, as done above. However the resulting CCN number concentrations are much more homogeneous over the domain. Concentrations typically vary by around a factor of 2 over the domain. The temporal variability over the whole time period, on the other hand, is larger, as shown in the bottom panel of Fig. 5. However, if shorter time periods

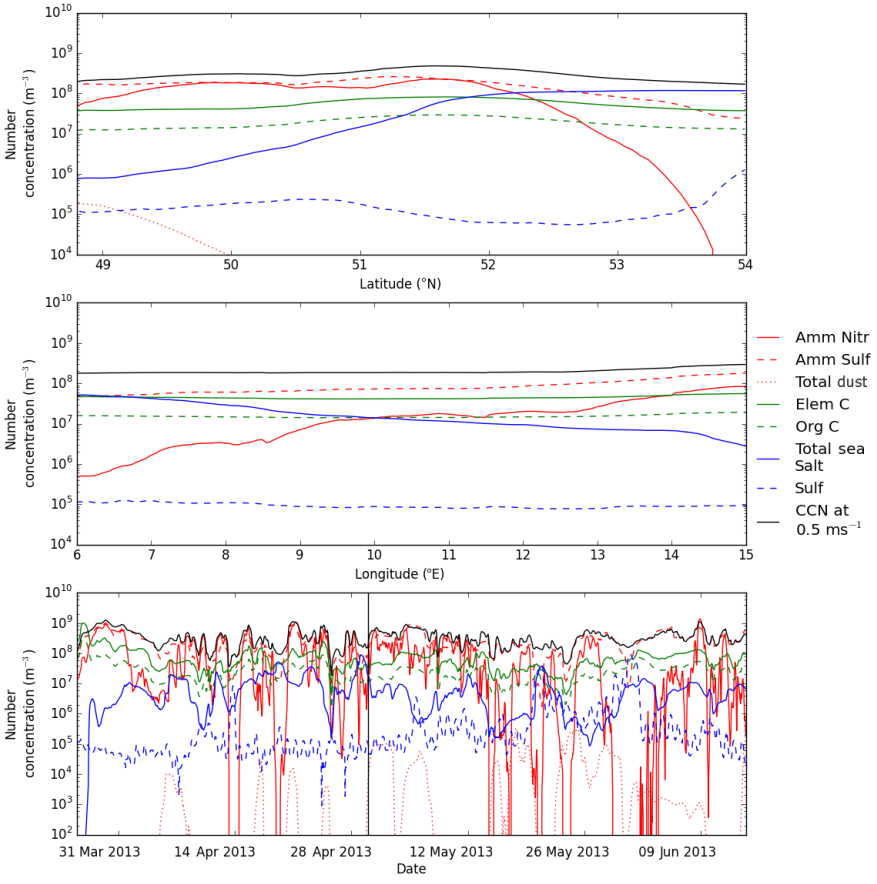

Figure 5. Latitudinal (top) and longitudinal (middle) median number concentration for aerosols and CCN at 0.5 m s^{-1} for 30 April 2013. Domain-wide median number concentration (bottom) for aerosols and CCN at 0.5 m s^{-1} for the HOPE campaign time period. The solid vertical line indicates the time period of the two upper panels.

of about 1 day are taken, this can be considered to be more constant.

Boucher et al. (2013) also notes that there is low confidence in estimates of the anthropogenic fraction of CCN. In an effort to address this, the fraction that each individual aerosol species contributes to the calculated CCN concentrations is shown in Table 2. Here, CCN concentrations are calculated at a vertical velocity of 0.5 m s^{-1} and, according to Abdul-Razzak et al. (1998), this gives an activated fraction of approximately 0.1 for ammonium sulfate aerosols at 10 °C and 800 hPa. The same activated fraction is found at a supersaturation of approximately 0.2 %, which is commonly used by other authors to calculate CCN concentrations (Pierce and Adams, 2009; Wang and Penner, 2009). Of course this depends on the particular aerosol species, aerosol size, and thermodynamic conditions; however it indicates that the results in Table 2 are roughly comparable to those of other studies.

Table 2 indicates that the CCN number concentrations over Germany are dominated by CCN formed on anthropogenic aerosols. Specifically, ammonium sulfate and sulfate dominate CCN production in the upper levels, and ammonium nitrate and ammonium sulfate are the dominant aerosols in the lower levels. Although elemental carbon aerosols have a high concentration throughout the atmosphere, their contribution to CCN is negligible due to the very low hygroscopicity. The sea salt aerosols, which are the most hygroscopic, only play a minor role in CCN production over the continent. Organic carbon and desert dust aerosols have the same hygroscopicity; therefore the differences in CCN production are due to differences in the number concentrations of aerosols.

These results are outside the upper bound of estimates of the global mean anthropogenic fraction of CCN. Boucher et al. (2013) combine numerous studies to suggest the anthropogenic fraction of CCN is between 0.25 and 0.66; however the authors did note the large uncertainties and large regional differences in these estimates. Furthermore, sea salt aerosols would be a larger contributor to the global mean, and this would act to reduce the anthropogenic fraction of CCN compared to the largely continental conditions over Germany. Given that when there are errors in modelled aerosol mass concentrations, the model is biased to lower values compared to the observations, and Table 2 shows the relative contribu-

Table 2. Percentage contribution of each aerosol species to total CCN number concentrations at 0.5 m s^{-1} for 507 and 906 hPa. Each aerosol species is indicated as either anthropogenic (A) or natural (N).

	Amm nitr (A)	Amm sulf (A)	Elem C (A)	Sulf (A)	Total A
507 hPa	3.55	42.96	1.57×10^{-5}	32.58	79.09
	Dust (N)	Org C (N)	SS (N)		Total N
507 hPa	2.23×10^{-2}	16.89	3.99		20.91
	Amm nitr (A)	Amm sulf (A)	Elem C (A)	Sulf (A)	Total A
906 hPa	46.18	46.53	1.26×10^{-7}	2.66×10^{-2}	92.74
	Dust (N)	Org C (N)	SS (N)		Total N
906 hPa	1.21×10^{-3}	5.24	2.02		7.26

tion of modelled aerosols to total CCN. The errors should not affect these results strongly.

5 Parameterization development

The previous section demonstrated that the median vertical profile of CCN number concentrations can be considered representative of the conditions over Germany during the HOPE campaign if short time periods of 1 day are considered. Here, a parameterization of CCN concentrations is constructed, which is a function of the atmospheric pressure and the vertical velocity. Using the parameterization provided by Abdul-Razzak and Ghan (2000), median CCN number concentrations were calculated at 40 different vertical velocities for each time step of modelled aerosol data. The average over all time steps in 1 day was computed, and this was used to define a series of best fit functions. In this way, aerosol physical and chemical properties are included through the use of Abdul-Razzak and Ghan (2000), as well as the important dependence on the vertical velocity at various pressure levels.

Figure 6 shows the CCN activation spectrum at each of the 32 pressure levels, for 1 day during HOPE, as well as the average of all data used in this study. Pressure levels closer to the ground have larger CCN number concentrations. The characteristic shape of this activation spectrum can be described at each pressure level by the following relation:

$$\mathrm{CCN}(w) = A \times \arctan(B \times \log(w) + C) + D, \quad (1)$$

where $\log(w)$ is the natural logarithm of vertical velocity in m s^{-1}. This best fit function for each pressure level is shown as the red lines in Fig. 6. The fitting was performed by means of a non-linear least squares method, where the data are first approximated by a model, and the model parameters are refined through successive iterations which minimize the errors between the data and model. In Fig. 6, low vertical velocities correspond to low supersaturations, and as a result very

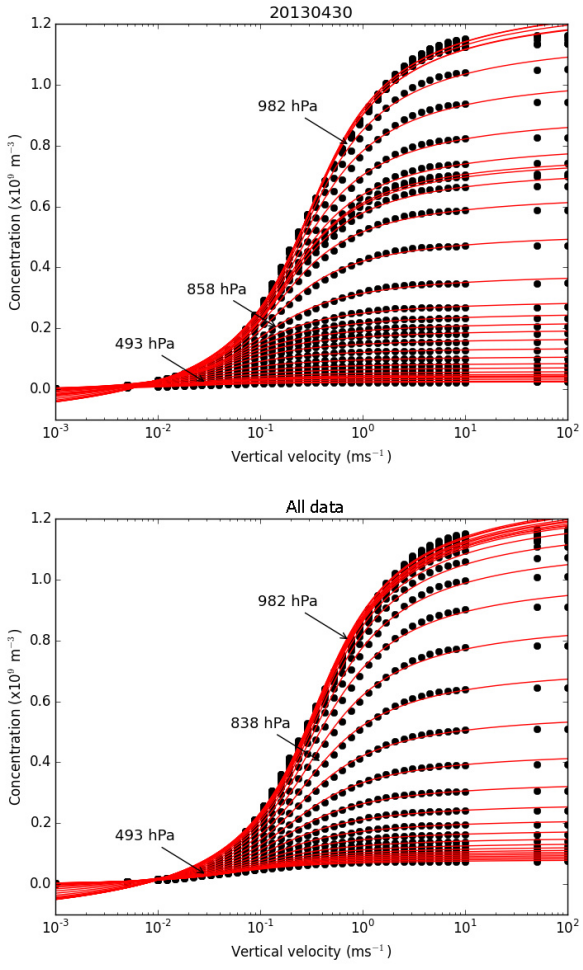

Figure 6. CCN activation spectrum for 30 April 2013 (top) and all data (bottom). Black circles represent the model data, red lines are the best fit functions.

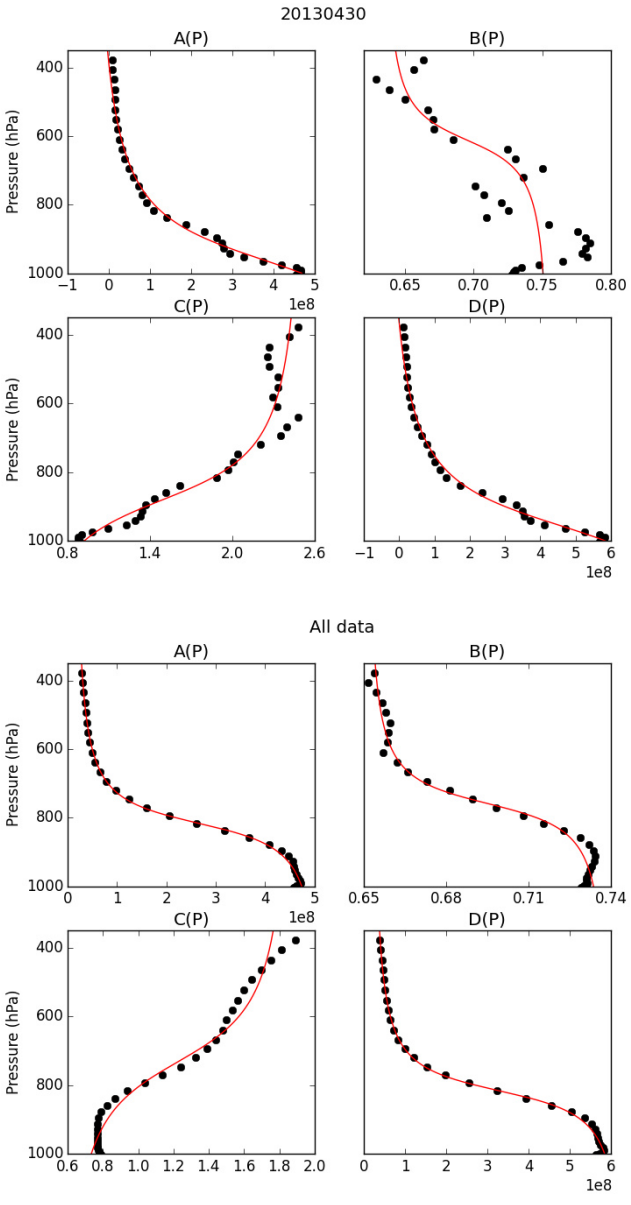

Figure 7. Parameters A, B, C, and D as a function of pressure for 30 April 2013 (top) and all data (bottom). Black circles represent the model data, red lines are the best fit functions.

few particles are activated. As the vertical velocity increases, an increasing number of particles are activated, until the activated fraction approaches 1 at high vertical velocities. This relationship is an inherent attribute of the Abdul-Razzak et al. (1998) parameterization and is best described by the arctan function.

This function provides a very good fit to the modelled activation spectrum, particularly in the range of vertical velocities between 0.01 and 50 m s^{-1}. At very small vertical velocities, the function can produce negative CCN number concentrations, particularly for pressure levels closer to the ground. This is the largest source of discrepancies between the parameterization and the modelled CCN data. The parameters A, B, C, and D act to control the scale, shape, and position of the curve at each pressure level and have a characteristic variation with pressure themselves, as shown in Fig. 7.

Curves of the following form can be fit to each of these parameters:

$$A(P) = a_1 \times \arctan(b_1 \times P + c_1) + d_1 \quad (2)$$

$$B(P) = a_2 \times \arctan(b_2 \times P + c_2) + d_2 \quad (3)$$

$$C(P) = a_3 \times \arctan(b_3 \times P + c_3) + d_3 \quad (4)$$

$$D(P) = a_4 \times \arctan(b_4 \times P + c_4) + d_4, \quad (5)$$

where P is pressure in Pascals. In this series of equations, pressure is used as the vertical coordinate. The shape of these curves is influenced by the structure of the atmosphere, and in some cases a different functional form may be more appropriate than Eqs. (2) to (5). The key to developing a parameterization using this technique is that a function of any type can be fit to these parameters. In some examples examined during HOPE, the fit for the B parameter can be poor. This often occurs when there is a second increase in this parameter above about 700 hPa. However, the influence this parameter has on the final parameterized CCN concentrations is small, and it can be seen from the bottom panels of Fig. 7, that on average the fit provided by Eqs. (2) to (5) is very good. Combining Eqs. (1) to (5), the CCN number concentrations (m^{-3}) are defined as follows:

$$\mathrm{CCN}(w, P) = A(P) \times \arctan(B(P) \times \log(w) + C(P)) + D(P), \quad (6)$$

where the 16 parameters a_1 to d_4 must be defined for each time period. These parameters are provided in Table A1 of Appendix A for each day of HOPE, as well as the mean over the whole time period. Users must first decide which CCN profile suits the needs of their simulation and select the appropriate fit parameters. The domain mean surface pressure, temperature, and vertically integrated specific humidity given in Table A2 may assist in this regard, if users wish to apply them to days not parameterized. The mean CCN profile can be employed for longer simulations not wishing to include daily variability.

Figure 8 shows the parameterization compared to CCN number concentrations calculated directly from the modelled aerosol data, at multiple vertical velocities. As can be seen, discrepancies between the parameterized CCN concentrations and those calculated directly from the model data are most significant at vertical velocities less than about 0.02 m s^{-1}, and pressure levels lower than 800 hPa. However, at vertical velocities greater than about 0.1 m s^{-1}, the parameterization derived above provides an excellent fit for the modelled CCN concentrations. These larger vertical velocities are most relevant for conditions within clouds. In order

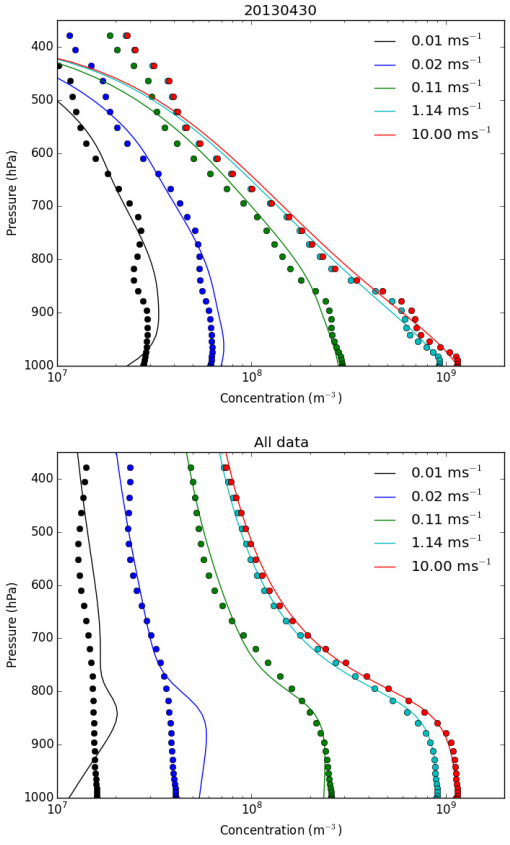

Figure 8. Modelled (circles) and parameterized (lines) CCN concentrations at multiple vertical velocities for 30 April 2013 (top) and all data (bottom).

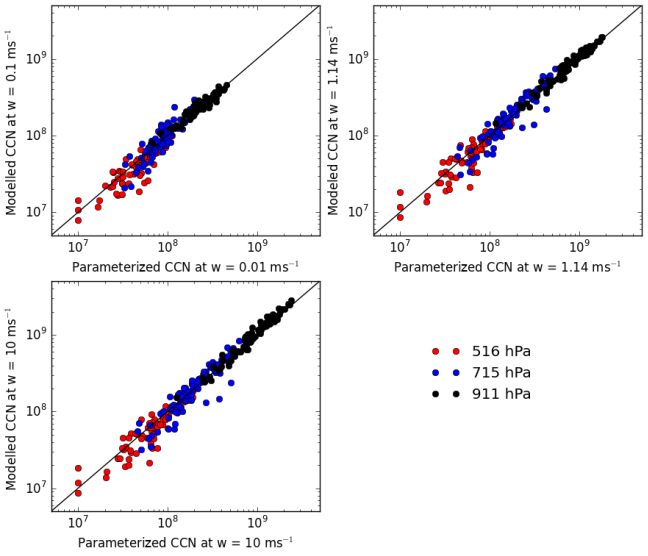

Figure 9. Scatter diagrams of modelled CCN number concentrations against parameterized CCN number concentrations, for $w =$ 0.01 (upper left), 1.14 (upper right), and 10 m s^{-1} (lower left), and for 516 (red), 715 (blue), and 911 hPa (black).

to prevent unrealistically low CCN number concentrations, it is recommended to implement a minimum CCN concentration of 10^7 m^{-3}.

This approach to parameterizing CCN concentrations has an advantage over other traditional methods. The CCN parameterization developed by Segal and Khain (2006) assumes a constant CCN concentration up to a specified height, above which the concentration decreases exponentially. This would only be a suitable representation in the case of a well-mixed boundary layer, with no aerosol and, therefore, no CCN production in the upper levels. The parameterization developed above is flexible enough to account for an atypical vertical distribution of CCN. For example, the top panel of Fig. 8 shows no well-mixed region, instead an almost linear decrease in CCN concentrations from the surface through to the mid-troposphere. Furthermore, Fig. 4 implies that sulfate aerosols can be produced in the upper levels; therefore the rate of decrease in CCN number concentrations above the boundary layer may not be exponential. It is suggested that the vertical profile of CCN number concentration obtained through this new parameterization provides a more accurate representation.

Figure 9 shows scatter diagrams of the modelled CCN number concentrations against the parameterized CCN number concentrations for 3 pressure levels and 3 vertical velocities. Overall, there is no significant bias in the parameterized CCN number concentrations. At high pressures, the agreement between the parameterized and modelled number concentrations is excellent, but the differences between the two increase with decreasing pressure. At 1.14 m s^{-1}, the average absolute magnitudes of the difference between the parameterized and modelled number concentrations are 8, 22, and 22 % of the modelled concentrations at 911, 715, and 516 hPa respectively. The three points at 516 hPa and a parameterized number concentrations of 1×10^7 m^{-3} would have very low number concentrations according to Eq. (6), hence the values must be adjusted to a minimum of 1×10^7 m^{-3}. These profiles are from 9 to 11 April 2013.

To further quantify the quality of the fit, the normalized root mean squared error (nRMSE) for each profile was computed, as shown in Table A2. The maximum nRMSE is 0.1930 for 3 June 2013, the minimum is 0.0127 for 1 April 2013, and the mean nRMSE over all days is 0.0555, which implies mean errors of 5.55 %. A qualitative inspection of the residuals, defined as Abdul-Razzak and Ghan (2000) – Eq. (6), was also made (not shown). The residuals were largest in the lower troposphere, but are still small relative to the maximum concentrations. This indicates that there is a small amount of variability in CCN concentrations that Eq. (6) does not capture. In the upper levels, the residuals are much closer to zero, which indicates that the form of the parameterization is appropriate for capturing the main features in the vertical distribution of CCN.

6 Conclusions

The COSMO–MUSCAT model was used to simulate the generation and transport of aerosols to Europe during the HOPE campaign. An evaluation of the modelled aerosol concentrations with available observations shows good agreement. The mass concentrations and temporal variability of ammonium sulfate, ammonium nitrate, and sea salt concentrations are in very good agreement with observations from Melpitz. Total $PM_{2.5}$ concentration is underestimated by the model by a factor of about 2. The size distribution from the model also agrees well with observations; however there is a slight underestimate at smaller and larger particle sizes.

From these aerosol concentrations, CCN number concentrations were calculated. The analysis demonstrated that while there may be large variability in aerosol concentrations throughout the domain considered here, the spatial variability of the resulting CCN concentrations is significantly lower, typically only varying by a factor of 2. There is, on the other hand, a larger amount of temporal variability over the time period. This implies that the median vertical profile of CCN number concentrations is most representative of the conditions over Germany if short time periods are considered.

The anthropogenic fraction of CCN was found to be large over continental Germany, at over 90 % near the surface, decreasing to about 80 % in the mid-troposphere. This is larger than estimates of the global mean and demonstrates the significant impact that anthropogenic aerosols have on cloud properties.

A parameterization of CCN number concentrations was developed, using a series of best fit functions to capture the dependency of CCN activation on vertical velocity at different pressure levels. In this parameterization, the influence of aerosol physical and chemical properties on CCN are included through the prior use of a detailed aerosol activation scheme. The parameterized CCN number concentrations compare well to the number concentrations calculated directly from the modelled aerosol data, except at very low vertical velocities and pressure levels close to the ground. This represents a new approach for parameterizing CCN for use in models, which to the authors knowledge has not been demonstrated before. As long as the technique provides adequate fits of all the free parameters in Eq. (6), this technique can be employed to parameterize CCN in other regions and over other time periods.

7 Data availability

Data used in this manuscript can be provided upon request by email to the corresponding author, Luke Hande (luke.hande@kit.edu).

Appendix A

Table A1. Parameters defining the CCN parameterization.

Date (yyyy-mm-dd)	a_1	b_1	c_1	d_1
2013-03-26	257027511.629	0.000199979502434	−17.6117849009	422546964.512
2013-03-27	257259587.478	0.000201760653742	−17.0754515981	458225862.794
2013-03-28	248134036.277	0.000248771867112	−19.8502078315	486429124.702
2013-03-29	293002066.039	0.000225778435403	−17.3399883006	557584166.907
2013-03-30	252381141.108	0.000128527088931	−10.0148105244	425988267.377
2013-03-31	315995778.379	0.000105411525029	−8.52132974576	476826117.331
2013-04-01	383647486.647	$9.53987511704 \times 10^{-5}$	−8.32043216657	570523268.512
2013-04-02	324811271.228	0.000138642834665	−12.2490672445	530652188.373
2013-04-03	223154550.008	0.000210211401757	−18.2301131592	389572102.855
2013-04-04	185174471.514	0.00027916990502	−24.9758011901	312654653.088
2013-04-05	123965671.328	0.000220481723183	−20.2930529312	214063096.868
2013-04-06	186141937.179	0.000119207983665	−10.6880203951	289075639.249
2013-04-07	197619469.896	0.000195683880524	−16.6673454676	306111694.706
2013-04-08	228555620.453	0.000209968372046	−18.0177227325	353752154.783
2013-04-09	165782282.315	0.000158862778002	−13.3344716637	230965254.836
2013-04-10	149088253.239	0.000197799417401	−16.8329323519	210898751.656
2013-04-11	188933606.377	0.000205926861534	−18.7422637505	277465364.811
2013-04-12	151501378.329	0.000154496611164	−13.3548084787	222893897.281
2013-04-13	182711318.548	0.000186202391181	−15.4762408599	266493038.479
2013-04-14	165170320.037	0.000278508634965	−26.9803029196	260454659.599
2013-04-15	195696398.475	0.000105519547855	−9.51386317268	287279759.576
2013-04-16	224420005.659	0.000293961293006	−23.3619212815	350287206.787
2013-04-17	132585467.481	0.00026097002081	−22.2848137664	220276289.561
2013-04-18	66896808.8009	0.000622874606996	−47.5770620781	149054005.269
2013-04-19	70902191.9176	0.000268682081376	−22.3654923985	113755021.935
2013-04-20	54046034.4806	0.000463840088873	−39.6472498837	93778930.966
2013-04-21	237046050.889	0.000197584785429	−15.7411031906	354983011.683
2013-04-22	350703557.487	0.000248652491121	−19.1756371885	535342752.709
2013-04-23	277648946.464	0.000220951487302	−18.756838732	417530444.244
2013-04-24	326536851.625	0.000476307032206	−40.0176304001	520404849.951
2013-04-25	297051358.433	0.000160822913339	−12.9411417647	437962207.588
2013-04-26	123186926.017	0.000195179520486	−13.4949151996	183690869.78
2013-04-27	110210087.645	0.000239022945279	−21.8073672723	169437053.325
2013-04-28	164323035.999	0.00015523807202	−13.5145674577	236667368.805
2013-04-29	242468712.867	0.0001916705582	−16.2115926716	355241545.175
2013-04-30	268062705.206	$9.00228432568 \times 10^{-5}$	−8.67002079484	369899109.621
2013-05-01	102511887.928	0.000421989534664	−34.118007519	167341263.238
2013-05-02	188914931.006	0.000531227091679	−41.6626456765	299914013.763
2013-05-03	166534415.574	0.000345442088574	−27.3432677906	257750601.317
2013-05-04	170209024.489	0.000349594756448	−27.9177073888	264146914.747
2013-05-05	169785924.886	0.000831242458893	−66.8062397787	285125428.499
2013-05-06	278790529.473	0.000451534894898	−34.9583814579	443180679.414
2013-05-07	242323023.311	0.000233685933182	−17.7939128097	367463885.465
2013-05-08	274335739.495	0.000213306540004	−17.0245331362	412727950.786
2013-05-09	113333109.973	0.000509886806569	−38.659883261	195376416.716
2013-05-10	105744547.317	0.000538143118997	−42.6695357287	172643018.723
2013-05-11	162385382.85	0.000332727679016	−26.8845754909	251110679.598
2013-05-12	102248916.147	0.000541014965278	−43.8361853001	175912999.174
2013-05-13	143779878.725	0.000155656177112	−13.6193322737	227494184.849

Table A1. Continued.

Date (yyyy-mm-dd)	a_1	b_1	c_1	d_1
2013-05-14	118394120.321	0.000336419574937	−28.0940496016	211132273.023
2013-05-15	137515734.708	0.000205753839294	−16.8745414588	227625697.257
2013-05-16	161976926.272	0.000200490706083	−16.4967738319	240382761.941
2013-05-17	177831147.397	0.000101960076261	−9.76398595204	260133006.929
2013-05-18	104881119.861	0.000246405889005	−21.9696591509	182569272.058
2013-05-19	179777743.64	0.0002080697608	−18.6108519411	285371721.017
2013-05-20	118821569.691	0.000222886738303	−18.7921495959	204363017.191
2013-05-21	165508396.77	0.000114815803897	−9.84950957879	250730495.161
2013-05-22	70615209.8813	$3.32596702867 \times 10^{-5}$	−2.98203668112	102740204.691
2013-05-23	33784879.7638	0.000246796867986	−20.6103783055	95065841.3682
2013-05-24	69249667.1912	0.000191067256933	−16.0354837343	133852326.6
2013-05-25	115027389.491	$7.61382715981 \times 10^{-5}$	−7.37537621712	172994343.375
2013-05-26	37450539.3977	0.000368115275095	−33.830244913	72896973.5148
2013-05-27	101409398.615	0.000128765200546	−10.8783417297	159533090.217
2013-05-28	238929584.969	$8.95306448836 \times 10^{-5}$	−7.49168205554	314416272.56
2013-05-29	238883906.14	0.000151184644169	−12.2144440358	342930672.175
2013-05-30	174563406.955	0.000213620483956	−17.1817084836	289090000.942
2013-05-31	112478707.879	0.000142127082463	−11.0733353463	194024530.85
2013-06-01	338306772.546	$3.61392403177 \times 10^{-5}$	−4.09357557336	439858074.785
2013-06-02	13434965.7592	0.000925991878154	−83.7326610938	112739974.004
2013-06-03	30168723.3708	0.000495944658031	−44.0243294791	126010850.256
2013-06-04	97237112.3611	$7.26358090841 \times 10^{-5}$	−6.24517522307	190489849.419
2013-06-05	82203983.0014	0.000116274085792	−9.47442018757	176075128.011
2013-06-06	86173034.7384	0.000383182474213	−29.5769436462	191563430.341
2013-06-07	135064790.26	0.000388462942097	−29.6327517089	263840022.66
2013-06-08	165886739.585	0.000416275919247	−31.8020906757	315914626.231
2013-06-09	132133978.232	0.000232190223914	−17.8646334752	248371577.344
2013-06-10	118866967.784	0.000150818334962	−12.5455428262	212616425.951
2013-06-11	192876867.075	0.000221833101314	−17.4557128001	329976771.525
2013-06-12	331533472.985	0.000304652092061	−24.1376489102	538001096.899
2013-06-13	121083645.226	0.000303472188084	−25.3943799881	232222942.427
2013-06-14	101662155.522	0.00128461981711	−104.950293772	217280192.35
2013-06-15	125114045.253	0.00164830616793	−127.12314395	257013581.432
2013-06-16	85205897.7055	0.00079239927885	−65.1012178105	179403546.146
All Data	163284250.556	0.000180120078194	−14.7056272648	265362821.369

Date (yyyy-mm-dd)	a_2	b_2	c_2	d_2
2013-03-26	−0.029814839848	0.000163327802941	−10.4068100415	0.6769189828
2013-03-27	−0.0325852534009	0.000276069056108	−12.8380343988	0.757535237671
2013-03-28	−0.0119185706848	−0.00292288814881	232.270889355	0.757360519289
2013-03-29	−0.0188580074505	−0.00373049506288	286.859628744	0.781750394241
2013-03-30	−0.0229861235094	−0.00337830269291	251.75895753	0.775685065229
2013-03-31	0.0151256499305	0.0011388666053	−89.3979117485	0.770358316613
2013-04-01	0.0189951868813	0.000514633362646	−44.3398908414	0.756453767604
2013-04-02	0.0155879769898	0.000531979507126	−46.1373434796	0.764685259415
2013-04-03	0.0160831365488	0.0103282444131	−866.529699837	0.7433128158
2013-04-04	0.0143849209764	0.0498638233939	−4377.47891107	0.739026494198
2013-04-05	0.00760368959733	0.0251201147357	−2329.11898411	0.720049432984
2013-04-06	0.0111568649285	0.00411606061595	−387.334321658	0.72518267401
2013-04-07	0.0113855040451	0.00828281993024	−710.993665143	0.719959884286
2013-04-08	0.0130949075301	0.0013770247057	−118.658153493	0.731955333102
2013-04-09	−0.0501207426563	0.000111624214554	−5.90812593792	0.796894769498
2013-04-10	−0.044333962825	0.00022764067347	−15.8680346727	0.776901997407
2013-04-11	−0.0180182385636	0.00851026594054	−634.547291807	0.743204805806

Table A1. Continued.

Date (yyyy-mm-dd)	a_2	b_2	c_2	d_2
2013-04-12	−0.0348227896411	0.000147753516038	−6.48537246095	0.745624009049
2013-04-13	0.00794151096456	0.00107642641128	−85.8373757326	0.715935780732
2013-04-14	0.038693640436	0.000410451577778	−20.1021023967	0.668367404449
2013-04-15	0.126571719449	$3.80199857817 \times 10^{-5}$	−1.26567516392	0.571940577379
2013-04-16	0.0442953079199	0.000245814787742	−17.7011580749	0.703578821734
2013-04-17	0.0614177873846	$7.5554755103 \times 10^{-5}$	−5.69776314638	0.649860475407
2013-04-18	0.0557206584146	0.00049403679403	−34.1444505909	0.598701901089
2013-04-19	−0.0107608339541	0.000510072770769	−35.8890069504	0.702770937226
2013-04-20	−0.0340616320637	0.00589359697711	−325.81712188	0.731052515565
2013-04-21	0.0196400746521	0.000599383945072	−44.1324325861	0.70371451307
2013-04-22	0.0527699977656	0.000248259433057	−17.2667172986	0.72497660722
2013-04-23	0.047931663221	0.000607996993056	−47.3945691166	0.704347498783
2013-04-24	0.0453353322421	0.000623698149368	−50.6528180808	0.709324351895
2013-04-25	65.4475055841	0.00580511453284	−28.9358471088	−101.913230262
2013-04-26	0.0104486344817	0.00122908611961	−91.5241853954	0.720829904429
2013-04-27	−0.0286421389331	0.00028807078372	−22.0346749088	0.757250590893
2013-04-28	−0.0274886165954	0.00377253418203	−230.845564031	0.752272034805
2013-04-29	25.5809712348	0.000282584826916	32.8793907769	−38.9937575255
2013-04-30	−0.0368311926571	−0.000174258591758	10.7064355564	0.6952993282
2013-05-01	0.0135912432763	0.00116628079855	−99.2069395798	0.702624978333
2013-05-02	0.0248350654338	0.00134800400185	−100.069936639	0.721198815048
2013-05-03	−0.0153572204661	−0.00257925380382	204.769223034	0.724407784298
2013-05-04	−0.0155709142123	−0.00268073465594	212.924912417	0.724410206287
2013-05-05	0.0493431363349	0.00255746079276	−197.216212945	0.681033689362
2013-05-06	0.0304348752283	0.00138822910198	−107.67165669	0.739122705985
2013-05-07	−0.0189563211661	−0.00193158996003	142.888007811	0.743541868199
2013-05-08	−0.0204945766538	−0.000732603490207	55.5005987103	0.747655947116
2013-05-09	0.0300211673167	$7.7947799912 \times 10^{-5}$	−5.68853442875	0.722837967764
2013-05-10	−0.0213618854837	0.000274733904033	−17.028199312	0.743374798773
2013-05-11	−2.46552737502	0.0151246299239	−1582.41924306	−3.12072758678
2013-05-12	−0.0139017663139	0.00027851620683	−26.8682695389	0.714771501715
2013-05-13	0.0124283474368	0.000545650574569	−42.0000886773	0.697747611773
2013-05-14	0.0034283474368	0.000545650574569	−42.0000886773	0.697747611773
2013-05-15	−0.0367444689868	−0.000122747784463	10.5573007709	0.725675639967
2013-05-16	−0.810832542971	0.00576822448077	−640.398614387	−0.506710196986
2013-05-17	0.0234593664171	0.00102200286985	−97.493789532	0.76298549245
2013-05-18	0.0374535870591	$4.46584613895 \times 10^{-5}$	−2.64686634671	0.722042807921
2013-05-19	0.0129138591047	0.000520191639983	−47.1399467981	0.726974314612
2013-05-20	0.0399072344891	$5.36824439419 \times 10^{-5}$	−5.15883256757	0.746774023727
2013-05-21	0.00916153210837	0.0227872535083	−2000.5631296	0.730351283666
2013-05-22	−0.00867734260577	0.000878994804728	−54.5253166078	0.688136048799
2013-05-23	−0.084237316917	$-3.51587495995 \times 10^{-7}$	−1.46957040783	0.594308505026
2013-05-24	−0.00979403232467	0.001467664618	−72.2430777115	0.708502064111
2013-05-25	−0.1	5×10^{-5}	−0.5	0.83
2013-05-26	0.0226974956012	−0.000287634445498	25.1370934599	0.7246471921
2013-05-27	−0.00900416329567	0.0049821811569	−371.553867706	0.723009419426
2013-05-28	0.00452308088149	0.00886821690033	−834.202826692	0.747028286906
2013-05-29	−0.00735146323438	−0.921419025165	77260.9872538	0.748615624012
2013-05-30	−0.0213661981303	−0.000869381872845	65.5156529736	0.723557314935
2013-05-31	0.0156975384075	0.000927882265059	−69.8025212366	0.714998416504
2013-06-01	0.0119317574675	0.00266166236376	−198.324400697	0.692168966081
2013-06-02	0.0197813156726	0.00148349415601	−130.052548417	0.675923345178
2013-06-03	0.010118651257	−0.000978730377931	39.631928973	0.674753205687
2013-06-04	0.0112288905438	0.00213132765181	−174.76139083	0.662941933206

Table A1. Continued.

Date (yyyy-mm-dd)	a_2	b_2	c_2	d_2
2013-06-05	0.0121120858222	0.00074709092356	−60.0364656402	0.676774244876
2013-06-06	0.0154334027655	0.024281754693	−1871.23983096	0.696513907984
2013-06-07	0.0251669347664	0.00051606046222	−38.4607550706	0.722091560856
2013-06-08	0.0432657151129	0.000406591616308	−30.4276024142	0.75392995781
2013-06-09	0.0381896488685	0.000337345832544	−25.3217372648	0.744838180739
2013-06-10	0.0250429932744	0.000562960816431	−47.862698352	0.720779691293
2013-06-11	0.0384101319177	0.000386555829788	−27.7369231426	0.717952241602
2013-06-12	0.0459899436012	0.000844692260638	−60.9483594953	0.73761297588
2013-06-13	−0.020158885649	−0.0276287029505	2256.96907061	0.713505498794
2013-06-14	−0.0113154472794	−0.002921470433	226.028584109	0.704349149996
2013-06-15	−0.0187435029412	−0.00111456487272	81.7455206955	0.708851574533
2013-06-16	0.00408842837182	−0.00716541146274	332.112579081	0.70950778351
All Data	−0.0288027446725	−0.000171569387007	13.0270839469	0.695246510346

Date (yyyy-mm-dd)	a_3	b_3	c_3	d_3
2013-03-26	−1.25999010727	$2.68241230633 \times 10^{-5}$	−1.72213638658	1.65350478005
2013-03-27	−1.7839755869	$1.50929337952 \times 10^{-5}$	−0.837612435568	1.85077964544
2013-03-28	−146.099540152	0.000225138533191	22.1232658493	226.964569092
2013-03-29	−1.34131727013	$2.50404007492 \times 10^{-5}$	−1.09710211005	1.97401126273
2013-03-30	−373.973073375	0.0022301585943	42.4980960204	586.904883742
2013-03-31	−1.32071946789	$2.10784161196 \times 10^{-5}$	−1.44735197002	1.50783743906
2013-04-01	−595.988540448	0.00156838963697	76.2162181865	934.332741347
2013-04-02	−429.287209778	0.00195353999206	43.2591431888	673.300179085
2013-04-03	−354.397239742	0.00307301913246	3.24827794838	556.439227008
2013-04-04	−722.862758695	0.00304393888477	82.1984554958	1134.66288854
2013-04-05	−333.95573167	0.000784293626916	51.1205832771	523.196754074
2013-04-06	−408.652449376	0.00210744511673	33.5160310077	641.285679271
2013-04-07	−0.931285878466	$4.62239563217 \times 10^{-5}$	−3.30289909524	1.73383064603
2013-04-08	−0.70989332512	$7.55580178287 \times 10^{-5}$	−5.81108685449	1.5574853692
2013-04-09	−1.28261872563	$6.96289413036 \times 10^{-5}$	−4.76372043972	2.40211987664
2013-04-10	−1.08990759738	0.000130523268638	−9.65260135541	2.25019366451
2013-04-11	−0.695966886536	0.000154729891348	−12.4511039248	1.73172754779
2013-04-12	−1.24717832619	$4.82341633583 \times 10^{-5}$	−3.32321347743	2.08047919673
2013-04-13	−0.882943394797	$8.03509209991 \times 10^{-5}$	−5.77611904313	1.81629983255
2013-04-14	−0.287194877967	0.000600945728595	−54.0848223318	1.42466992937
2013-04-15	−0.418486879565	0.000116279302557	−9.34929026635	1.27060902036
2013-04-16	−0.463181171817	0.000229124424724	−17.6024080361	1.29279832853
2013-04-17	0.222918696941	−0.000394632485796	34.0018788402	1.18445134078
2013-04-18	0.147889372175	−0.00164037984568	126.698112989	1.25228964998
2013-04-19	−0.60286179518	0.000183648686699	−14.6929427448	1.96169583431
2013-04-20	−239.2009653	0.00104803671278	16.9061486135	375.304688779
2013-04-21	−0.849345878016	$9.20681792757 \times 10^{-5}$	−5.61903889161	1.72632960381
2013-04-22	−0.714584192015	$9.21357895543 \times 10^{-5}$	−5.97479789522	1.37126784234
2013-04-23	−0.424938795281	0.000192261099352	−15.8346004825	1.20278591386
2013-04-24	−0.465259558225	0.000237161116198	−19.1049134773	1.08031121538
2013-04-25	−0.475503560527	0.000192355777417	−13.230688361	1.18762265562
2013-04-26	−0.691019498158	0.000139959391683	−7.99850700522	1.73153075465
2013-04-27	−0.81914143666	0.000119282661856	−10.0243823956	1.87746719768
2013-04-28	−0.860513412579	0.000129941958131	−8.72046968585	2.06156811575
2013-04-29	−0.615207577704	0.000119808650723	−9.44135316974	1.46338145959
2013-04-30	−0.68509594868	$9.07655415297 \times 10^{-5}$	−7.99865058891	1.49322380511
2013-05-01	−0.519654567659	0.000317800267516	−24.2286991499	1.7689389708

Table A1. Continued.

Date (yyyy-mm-dd)	a_3	b_3	c_3	d_3
2013-05-02	−1.11280140047	$6.61309288082 \times 10^{-5}$	−4.27951113912	2.00538429673
2013-05-03	−0.88579724448	0.000110564000686	−7.32585831853	1.98284339015
2013-05-04	−1.61464525376	$3.80749098093 \times 10^{-5}$	−2.1436750988	2.36446975491
2013-05-05	−0.943848160565	$6.36900365619 \times 10^{-5}$	−3.90882328996	1.8565436722
2013-05-06	−1.07934637213	$7.62165327465 \times 10^{-5}$	−4.74010349215	1.71873623378
2013-05-07	−1.36286264208	$4.04236815208 \times 10^{-5}$	−2.20999762053	1.8481752194
2013-05-08	−0.925933829895	$6.36315473856 \times 10^{-5}$	−4.38246112807	1.35966523239
2013-05-09	−0.378846961048	0.000429287390377	−31.5025875823	1.44685075948
2013-05-10	−0.501317389762	0.000240832427312	−17.5918818622	1.67320066174
2013-05-11	−0.53908011762	0.00024339432442	−18.7836022684	1.57130610445
2013-05-12	−0.402134260333	0.000391241509497	−31.0299472561	1.62070840147
2013-05-13	−0.288871536496	0.000280973683123	−23.4245054386	1.37866424205
2013-05-14	−0.276208791978	0.000520773251996	−43.3298210327	1.33971395101
2013-05-15	−0.513895360814	$8.87032633236 \times 10^{-5}$	−6.7520351196	1.27851494147
2013-05-16	−0.560269238461	0.000170241511331	−13.1700323447	1.32265526036
2013-05-17	−0.444450818361	$9.1000429623 \times 10^{-5}$	−7.21512256963	1.35172979657
2013-05-18	−0.431046664338	0.000115546206148	−9.96130554955	1.32730747833
2013-05-19	−0.393353450063	0.000173858132453	−14.235403816	1.24108992813
2013-05-20	−0.407133122621	$9.89756705673 \times 10^{-5}$	−7.62420964636	1.37204332133
2013-05-21	−1.06704378015	$3.16238550312 \times 10^{-5}$	−2.10909965547	1.70820098197
2013-05-22	0.2510147687	−0.0001695851547	7.56871998468	1.86473578811
2013-05-23	−64.5312765505	0.00194892982989	16.3110676014	102.580813222
2013-05-24	−1.32499731808	$1.36299598588 \times 10^{-5}$	−1.16960888077	1.40358746653
2013-05-25	−0.682952076821	$5.3403772624 \times 10^{-5}$	−2.679349403	2.08151597839
2013-05-26	−0.32371095904	0.000148330227646	−13.3141113038	1.66721014705
2013-05-27	−0.427495645381	0.00011677249743	−9.14350543479	1.43762910725
2013-05-28	−0.927383001908	$5.1673406534 \times 10^{-5}$	−3.34816420136	1.69833286141
2013-05-29	−0.883501696306	$6.47564972491 \times 10^{-5}$	−4.37389872681	1.61543660421
2013-05-30	−0.548098680953	$6.73303475323 \times 10^{-5}$	−5.12858774595	1.15082901139
2013-05-31	−0.333808236562	$7.62249200252 \times 10^{-5}$	−5.54005586951	1.16717121961
2013-06-01	−370.325906495	0.00359677728395	87.2231226264	581.821654579
2013-06-02	0.0823717404931	0.00477201837839	−390.188669834	1.3230371111
2013-06-03	0.135609478302	−0.000729429424034	33.9764068217	1.35421490863
2013-06-04	96.1299450025	−0.000738569484517	−51.4460304317	151.183926683
2013-06-05	77.9952592775	−0.000116237778984	43.7683935449	−119.169528436
2013-06-06	−132.792420633	0.0011597576875	32.1840335634	208.466060446
2013-06-07	−0.498814169354	$4.75358934694 \times 10^{-5}$	−3.05512740933	1.13789325174
2013-06-08	−0.306538568777	0.000251163616886	−18.0807183492	1.03227497804
2013-06-09	−0.285724374574	0.000218245524802	−15.0935485458	1.22397376321
2013-06-10	−0.374092574015	$7.6645726738 \times 10^{-5}$	−5.42099078016	1.35984067623
2013-06-11	−0.32529828655	0.000161996594323	−12.1604750317	1.09488722572
2013-06-12	−0.331937538165	0.000291377512412	−22.836799656	0.82718268609
2013-06-13	0.144601621176	−0.00045898983022	39.7459325336	0.961554360906
2013-06-14	−0.173194732078	0.000971333233174	−78.8987838138	1.10277014402
2013-06-15	−0.219682412065	0.000723465343821	−55.7467841028	1.07610272578
2013-06-16	−0.169997837704	0.000748813288464	−62.7335523194	1.13678591019
All Data	−0.436109722435	$7.71432656612 \times 10^{-5}$	−5.65244631785	1.22261713713

Table A1. Continued.

Date (yyyy-mm-dd)	a_4	b_4	c_4	d_4
2013-03-26	302649571.476	0.000202604673235	−17.8601818352	505395811.033
2013-03-27	309844331.918	0.000201553447317	−17.0889369229	558425882.48
2013-03-28	303587929.431	0.000251184401777	−20.0776058128	600415097.602
2013-03-29	358319870.576	0.000235307642443	−18.109198242	689285340.24
2013-03-30	306411494.19	0.000130502738578	−10.2047241636	525245208.824
2013-03-31	388602484.531	0.000106640142718	−8.63617368737	591782562.502
2013-04-01	476072376.341	$9.54062745542 \times 10^{-5}$	−8.34686788976	712002557.477
2013-04-02	400738826.224	0.000137261994404	−12.1441852379	657786306.277
2013-04-03	271154223.173	0.000211618554738	−18.375924686	477963001.566
2013-04-04	222005914.307	0.000288026568537	−25.7839773553	380103114.138
2013-04-05	146113683.536	0.000226728363976	−20.8773726066	258303073.087
2013-04-06	227357309.834	0.000119261373742	−10.6947244824	356992826.431
2013-04-07	241308439.109	0.000199317529083	−16.9672587029	378439187.206
2013-04-08	280111919.968	0.000209214019672	−17.9793642396	437741879.199
2013-04-09	201988263.429	0.000156175726257	−13.1195924886	282584675.128
2013-04-10	181147956.533	0.000200223115362	−17.0477941637	259133440.218
2013-04-11	228846926.496	0.000206978315709	−18.8460886402	338431888.439
2013-04-12	183631089.844	0.000153283558203	−13.226675174	272877803.21
2013-04-13	223513894.045	0.000185040047855	−15.4004918451	328717289.549
2013-04-14	199272578.736	0.000279851195086	−27.1229057226	318094162.339
2013-04-15	237825410.444	0.00010536947044	−9.49476557929	353051123.926
2013-04-16	275956307.198	0.000300567567101	−23.9183353439	434779360.181
2013-04-17	162262731.983	0.000262094428674	−22.3945772632	272763175.919
2013-04-18	82974586.1468	0.000610602786755	−46.5958976279	185410192.143
2013-04-19	88507472.6693	0.000259954512805	−21.6919376495	143754056.01
2013-04-20	68031395.0028	0.000449484526955	−38.3766131975	119230454.464
2013-04-21	292556220.931	0.000199286765133	−15.8844557948	440295202.466
2013-04-22	436323704.056	0.000253625683664	−19.6109292178	670747233.536
2013-04-23	341478481.841	0.000224876807177	−19.0903094313	517788768.446
2013-04-24	407017229.474	0.000487594856181	−40.9747483446	653016436.865
2013-04-25	368817155.294	0.000162747488109	−13.0976538218	546387196.913
2013-04-26	149721272.911	0.000203000520319	−14.0650317208	227118473.008
2013-04-27	136925775.74	0.000231690353715	−21.1078296939	210681864.227
2013-04-28	200772495.141	0.000157057847042	−13.646482707	291386102.455
2013-04-29	298588454.619	0.000193175186475	−16.3641258221	440534263.922
2013-04-30	321053687.393	$9.13903026692 \times 10^{-5}$	−8.74143108092	445375723.086
2013-05-01	125985285.773	0.000423966625778	−34.2688922351	207432107.013
2013-05-02	231487402.046	0.000539065575467	−42.2833148055	369926688.758
2013-05-03	203776163.79	0.0003437601979	−27.2333299684	317651818.018
2013-05-04	208338967.959	0.000346456469493	−27.6854907624	325702553.336
2013-05-05	207789963.508	0.000841796072708	−67.6622303188	351993627.965
2013-05-06	347418417.851	0.000448524359662	−34.7780924713	554135086.863
2013-05-07	299783172.592	0.000235981220195	−17.9925942326	457931647.005
2013-05-08	338853590.457	0.000222740166646	−17.7969628434	515122066.518
2013-05-09	138350731.516	0.000514433319282	−39.0494638988	242861950.818
2013-05-10	128460991.586	0.000542872119089	−43.0392477758	212376408.167
2013-05-11	197357722.636	0.000336170352883	−27.1769290538	308896495.572
2013-05-12	123438090.825	0.000551986537608	−44.7389812631	216939776.454
2013-05-13	173262903.075	0.000156157996316	−13.6719350276	279915831.861
2013-05-14	143307785.834	0.000341916985123	−28.5463023673	262248737.61
2013-05-15	171687143.506	0.000204960171235	−16.8430743062	288242524.489
2013-05-16	201124120.263	0.000199727851722	−16.4635685193	300436734.559
2013-05-17	216048762.633	0.000106256317825	−10.1785101296	321330376.197

Table A1. Continued.

Date (yyyy-mm-dd)	a_4	b_4	c_4	d_4
2013-05-18	127019310.246	0.000251878447586	−22.4725980735	225359020.405
2013-05-19	216139229.118	0.00021017737448	−18.8082043681	347954786.732
2013-05-20	142802725.584	0.00022408357457	−18.9053267444	250315544.354
2013-05-21	198870491.145	0.000117988992593	−10.139042474	307531288.823
2013-05-22	119432620.247	$2.43039229589 \times 10^{-5}$	−2.45632747881	157922601.653
2013-05-23	40255497.7353	0.000240171209101	−20.0498375634	122178037.277
2013-05-24	84013680.5912	0.000185305147735	−15.5745760304	167222406.923
2013-05-25	139565588.11	$7.67575081862 \times 10^{-5}$	−7.44485213716	214762700.992
2013-05-26	45132682.539	0.000361420216266	−33.2187435764	91005818.8736
2013-05-27	125197132.219	0.000124622035228	−10.5772038594	199654328.249
2013-05-28	291094314.932	$8.9376960719 \times 10^{-5}$	−7.48575179534	386048772.609
2013-05-29	290645572.411	0.000151162246919	−12.2349270666	420301468.84
2013-05-30	211052359.052	0.000220307547106	−17.7401273148	355841319.637
2013-05-31	135399096.842	0.000149711023647	−11.6821562186	240861848.761
2013-06-01	363627422.118	$3.56015208817 \times 10^{-5}$	−3.90250699652	473751252.603
2013-06-02	17968652.1809	0.000996972925851	−90.3011578173	144213180.306
2013-06-03	34016040.9651	0.000659872472514	−58.6294118973	162640835.637
2013-06-04	107395285.649	$8.78086171989 \times 10^{-5}$	−7.49763902659	234434320.597
2013-06-05	97909831.7666	0.000120067468126	−9.79807570646	221959838.278
2013-06-06	101756470.014	0.000456646803813	−35.3885995398	243262397.72
2013-06-07	161546476.68	0.00045407580782	−34.799243064	334220452.75
2013-06-08	203720180.213	0.000482356961371	−37.0202588174	405209487.11
2013-06-09	158442495.012	0.000269794457705	−20.8081300188	314318566.708
2013-06-10	141865122.829	0.000156947950278	−13.0695209013	263075585.99
2013-06-11	235733177.228	0.000230751828926	−18.1591128028	410288514.094
2013-06-12	415210885.836	0.000306663251406	−24.3201029806	674658738.154
2013-06-13	147073267.639	0.000309682098903	−25.9637042653	288869265.912
2013-06-14	120316710.214	0.00156899264184	−128.236691148	269620027.277
2013-06-15	150145578.989	0.00201136712971	−155.146937742	320889638.795
2013-06-16	102540538.867	0.000827094676632	−67.9962750683	224807397.25
All Data	199788909.439	0.000182424683277	−14.8932330043	328676886.493

Table A2. Normalized root mean square error (nRMSE), mean surface level pressure (MSLP), mean surface level temperature (MSLT), and mean integrated specific humidity (MISH).

Date (yyyy-mm-dd)	nRMSE	MSLP (hPa)	MSLT (K)	MISH ($\mathrm{kg\,kg^{-1}}$)
2013-03-26	0.058375	994.94	269.19	0.036122
2013-03-27	0.017049	993.75	269.51	0.035218
2013-03-28	0.031950	992.39	271.32	0.042123
2013-03-29	0.042817	987.85	272.93	0.055698
2013-03-30	0.041072	985.12	272.85	0.049807
2013-03-31	0.026466	988.42	272.43	0.048879
2013-04-01	0.012706	989.60	272.20	0.042296
2013-04-02	0.015847	990.95	272.05	0.036133
2013-04-03	0.022428	995.81	272.55	0.040998
2013-04-04	0.029187	994.44	272.86	0.048369
2013-04-05	0.041894	989.87	273.76	0.056840
2013-04-06	0.028730	993.01	274.46	0.057399

Table A2. Continued.

Date (yyyy-mm-dd)	nRMSE	MSLP (hPa)	MSLT (K)	MISH (kg kg^{-1})
2013-04-07	0.042814	999.94	274.21	0.048450
2013-04-08	0.026501	993.42	274.33	0.045672
2013-04-09	0.027307	985.84	275.56	0.057698
2013-04-10	0.076350	983.25	277.05	0.082018
2013-04-11	0.035495	985.89	278.18	0.088811
2013-04-12	0.034073	979.79	280.71	0.111517
2013-04-13	0.031444	986.42	279.62	0.090808
2013-04-14	0.037386	1001.00	279.63	0.096504
2013-04-15	0.047865	1001.01	282.66	0.108553
2013-04-16	0.034297	998.47	283.05	0.105820
2013-04-17	0.048725	999.54	284.12	0.112909
2013-04-18	0.088579	994.27	285.96	0.129610
2013-04-19	0.056774	996.16	283.23	0.087532
2013-04-20	0.079616	1004.96	279.29	0.068958
2013-04-21	0.111945	1004.65	278.71	0.065744
2013-04-22	0.055604	994.76	280.78	0.084171
2013-04-23	0.030981	994.66	281.98	0.089663
2013-04-24	0.015152	1002.46	281.75	0.091881
2013-04-25	0.075156	1002.65	284.35	0.121349
2013-04-26	0.121841	995.45	285.82	0.119089
2013-04-27	0.069493	984.92	281.90	0.115787
2013-04-28	0.088411	990.59	279.10	0.086938
2013-04-29	0.019399	993.20	280.35	0.088360
2013-04-30	0.038301	998.84	280.66	0.081556
2013-05-01	0.089889	1002.53	280.47	0.085800
2013-05-02	0.049596	999.81	282.07	0.106277
2013-05-03	0.046556	997.79	282.30	0.103677
2013-05-04	0.036288	994.96	282.31	0.095752
2013-05-05	0.086737	999.15	283.10	0.100445
2013-05-06	0.056681	1002.02	283.96	0.100265
2013-05-07	0.024180	997.57	285.96	0.130177
2013-05-08	0.052651	993.21	286.40	0.158999
2013-05-09	0.089977	991.31	287.25	0.150291
2013-05-10	0.106178	990.67	285.82	0.131964
2013-05-11	0.030124	994.27	283.82	0.112145
2013-05-12	0.067284	990.95	282.81	0.109726
2013-05-13	0.035593	993.67	281.24	0.098355
2013-05-14	0.037253	989.83	282.00	0.100587
2013-05-15	0.042805	985.28	283.20	0.113195
2013-05-16	0.034829	982.21	285.09	0.121981
2013-05-17	0.040659	978.31	286.23	0.148483
2013-05-18	0.026654	982.87	285.79	0.158700
2013-05-19	0.031035	988.83	284.13	0.124771
2013-05-20	0.023767	987.02	284.80	0.141561
2013-05-21	0.034408	989.34	283.91	0.125855
2013-05-22	0.050486	986.75	283.17	0.121123
2013-05-23	0.083085	988.22	279.80	0.075196
2013-05-24	0.080767	987.04	279.35	0.074817
2013-05-25	0.025863	990.34	281.01	0.094807
2013-05-26	0.031988	988.12	281.64	0.118393
2013-05-27	0.046164	985.93	281.49	0.107848
2013-05-28	0.046754	986.86	283.02	0.111575
2013-05-29	0.023271	980.41	283.99	0.126150
2013-05-30	0.032076	983.78	283.96	0.132437

Table A2. Continued.

Date (yyyy-mm-dd)	nRMSE	MSLP (hPa)	MSLT (K)	MISH ($kg\,kg^{-1}$)
2013-05-31	0.029660	983.61	284.88	0.149310
2013-06-01	0.028816	987.35	284.71	0.144646
2013-06-02	0.172472	992.77	283.76	0.130239
2013-06-03	0.193028	1000.69	282.29	0.105592
2013-06-04	0.042859	1000.92	282.77	0.109886
2013-06-05	0.035022	999.00	284.02	0.102547
2013-06-06	0.089583	999.76	284.51	0.108954
2013-06-07	0.114967	1000.78	286.25	0.124497
2013-06-08	0.095570	998.80	286.87	0.130221
2013-06-09	0.120264	993.08	286.41	0.131837
2013-06-10	0.033598	989.03	285.82	0.131744
2013-06-11	0.069040	992.94	285.16	0.111053
2013-06-12	0.037044	996.85	286.46	0.122328
2013-06-13	0.046920	995.83	289.15	0.174709
2013-06-14	0.129532	993.20	287.72	0.155478
2013-06-15	0.157566	995.72	286.45	0.115220
2013-06-16	0.084010	992.86	287.41	0.123394
All Data	0.055488	992.65	281.37	0.100991

The Supplement related to this article is available online at doi:10.5194/acp-16-12059-2016-supplement.

Author contributions. Christa Engler, working with Ina Tegen, ran the COSMO–MUSCAT model, and performed the aerosol evaluation. Luke B. Hande, working with Corinna Hoose, developed the CCN parameterization. Luke B. Hande prepared the manuscript with contributions from all co-authors.

Acknowledgements. This work was funded by the Federal Ministry of Education and Research in Germany (BMBF) through the research programme "High Definition Clouds and Precipitation for Climate Prediction – HD(CP)^2" (FKZ: 01LK1204B). The authors wish to thank Geralad Spindler and Wolfgang Birmili for providing data used in the evaluation. An electronic version of the parameterization parameters is available as a supplement to this manuscript.

The article-processing charges for this open-access publication were covered by a Research Centre of the Helmholtz Association.

Edited by: H. Russchenberg
Reviewed by: two anonymous referees

References

Abdul-Razzak, H. and Ghan, S. J.: A parameterization of aerosol activation: 2. Multiple aerosol types, J. Geophys. Res.-Atmos., 105, 6837–6844, 2000.

Abdul-Razzak, H. and Ghan, S. J.: A parameterization of aerosol activation 3. Sectional representation, J. Geophys. Res.-Atmos., 107, AAC 1-1–AAC 1-6, doi:10.1029/2001JD000483, 2002.

Abdul-Razzak, H., Ghan, S. J., and Rivera-Carpio, C.: A parameterization of aerosol activation: 1. Single aerosol type, J. Geophys. Res.-Atmos., 103, 6123–6131, 1998.

Bellouin, N., Mann, G. W., Woodhouse, M. T., Johnson, C., Carslaw, K. S., and Dalvi, M.: Impact of the modal aerosol scheme GLOMAP-mode on aerosol forcing in the Hadley Centre Global Environmental Model, Atmos. Chem. Phys., 13, 3027–3044, doi:10.5194/acp-13-3027-2013, 2013.

Birmili, W., Stratmann, F., and Wiedensohler, A.: Design of a DMA-based size spectrometer for a large particle size range and stable operation, J. Aerosol Sci., 30, 549–553, 1999.

Birmili, W., Weinhold, K., Rasch, F., Sonntag, A., Sun, J., Merkel, M., Wiedensohler, A., Bastian, S., Schladitz, A., Löschau, G., Cyrys, J., Pitz, M., Gu, J., Kusch, T., Flentje, H., Quass, U., Kaminski, H., Kuhlbusch, T. A. J., Meinhardt, F., Schwerin, A., Bath, O., Ries, L., Wirtz, K., and Fiebig, M.: Long-term observations of tropospheric particle number size distributions and equivalent black carbon mass concentrations in the German Ultrafine Aerosol Network (GUAN), Earth Syst. Sci. Data, 8, 355–382, doi:10.5194/essd-8-355-2016, 2016.

Boucher, O., Randall, D., Artaxo, P., Bretherton, C., Feingold, G., Forster, P., Kerminen, V.-M., Kondo, Y., Liao, H., Lohmann, U., Rasch, P., Satheesh, S., Sherwood, S., Stevens, B., and Zhang, X.: Clouds and Aerosols. In: Climate Change 2013: The Physical Science Basis. Contribution of Working Group I to the Fifth Assessment Report of the Intergovernmental Panel on Climate Change, Intergovernmental Panel on Climate Change, Working Group I Contribution to the IPCC Fifth Assessment Report (AR5)(Cambridge Univ Press, New York), 2013.

Dipankar, A., Stevens, B., Heinze, R., Moseley, C., Zängl, G., Giorgetta, M., and Brdar, S.: Large eddy simulation using the general circulation model ICON, Journal of Advances in Modeling Earth Systems, 7, 963–986, doi:10.1002/2015MS000431, 2015.

Dusek, U., Frank, G. P., Hildebrandt, L., Curtius, J., Schneider, J., Walter, S., Chand, D., Drewnick, F., Hings, S., Jung, D., Borrmann, S., and Andreae, M. O.: Size matters more than chemistry for cloud-nucleating ability of aerosol particles, Science, 312, 1375–1378, 2006.

Engler, C., Rose, D., Wehner, B., Wiedensohler, A., Brüggemann, E., Gnauk, T., Spindler, G., Tuch, T., and Birmili, W.: Size distributions of non-volatile particle residuals ($D_p < 800$ nm) at a rural site in Germany and relation to air mass origin, Atmos. Chem. Phys., 7, 5785–5802, doi:10.5194/acp-7-5785-2007, 2007.

Ervens, B., Cubison, M., Andrews, E., Feingold, G., Ogren, J. A., Jimenez, J. L., DeCarlo, P., and Nenes, A.: Prediction of cloud condensation nucleus number concentration using measurements of aerosol size distributions and composition and light scattering enhancement due to humidity, J. Geophys. Res.-Atmos., 112, D10S32, doi:10.1029/2006JD007426, 2007.

Ervens, B., Cubison, M. J., Andrews, E., Feingold, G., Ogren, J. A., Jimenez, J. L., Quinn, P. K., Bates, T. S., Wang, J., Zhang, Q., Coe, H., Flynn, M., and Allan, J. D.: CCN predictions using simplified assumptions of organic aerosol composition and mixing state: a synthesis from six different locations, Atmos. Chem. Phys., 10, 4795–4807, doi:10.5194/acp-10-4795-2010, 2010.

Feingold, G.: Modeling of the first indirect effect: Analysis of measurement requirements, Geophys. Res. Lett., 30, 1997, doi:10.1029/2003GL017967, 2003.

Fountoukis, C. and Nenes, A.: Continued development of a cloud droplet formation parameterization for global climate models, J. Geophys. Res.-Atmos., 110, D11212, doi:10.1029/2004JD005591, 2005.

Ghan, S., Laulainen, N., Easter, R., Wagener, R., Nemesure, S., Chapman, E., Zhang, Y., and Leung, R.: Evaluation of aerosol direct radiative forcing in MIRAGE, J. Geophys. Res.-Atmos., 106, 5295–5316, 2001.

Gong, S.: A parameterization of sea-salt aerosol source function for sub-and super-micron particles, Global Biogeochem. Cy., 17, 1097, doi:10.1029/2003GB002079, 2003.

Hande, L. B., Engler, C., Hoose, C., and Tegen, I.: Seasonal variability of Saharan desert dust and ice nucleating particles over Europe, Atmos. Chem. Phys., 15, 4389–4397, doi:10.5194/acp-15-4389-2015, 2015.

Heinold, B., Tegen, I., Schepanski, K., Tesche, M., Esselborn, M., Freudenthaler, V., Gross, S., Kandler, K., Knippertz, P., Müller, D., Schladitz, A., Toledano, C., Weinzierl, B., Ansmann, A., Althausen, D., Muller, T., and Petzold, A.: Regional modelling of Saharan dust and biomass-burning smoke, Tellus B, 63, 781–799, 2011.

Hudson, J. G.: Variability of the relationship between particle size and cloud-nucleating ability, Geophys. Res. Lett., 34, L08801, doi:10.1029/2006GL028850, 2007.

Khvorostyanov, V. I. and Curry, J. A.: A simple analytical model of aerosol properties with account for hygroscopic growth: 1. Equilibrium size spectra and cloud condensation nuclei activity spectra, J. Geophys. Res.-Atmos., 104, 2175–2184, 1999.

Liu, X., Easter, R. C., Ghan, S. J., Zaveri, R., Rasch, P., Shi, X., Lamarque, J.-F., Gettelman, A., Morrison, H., Vitt, F., Conley, A., Park, S., Neale, R., Hannay, C., Ekman, A. M. L., Hess, P., Mahowald, N., Collins, W., Iacono, M. J., Bretherton, C. S., Flanner, M. G., and Mitchell, D.: Toward a minimal representation of aerosols in climate models: description and evaluation in the Community Atmosphere Model CAM5, Geosci. Model Dev., 5, 709–739, doi:10.5194/gmd-5-709-2012, 2012.

Mann, G. W., Carslaw, K. S., Ridley, D. A., Spracklen, D. V., Pringle, K. J., Merikanto, J., Korhonen, H., Schwarz, J. P., Lee, L. A., Manktelow, P. T., Woodhouse, M. T., Schmidt, A., Breider, T. J., Emmerson, K. M., Reddington, C. L., Chipperfield, M. P., and Pickering, S. J.: Intercomparison of modal and sectional aerosol microphysics representations within the same 3-D global chemical transport model, Atmos. Chem. Phys., 12, 4449–4476, doi:10.5194/acp-12-4449-2012, 2012.

Morrison, H., Curry, J., and Khvorostyanov, V.: A new double-moment microphysics parameterization for application in cloud and climate models. Part I: Description, J. Atmos. Sci., 62, 1665–1677, 2005.

Nenes, A. and Seinfeld, J. H.: Parameterization of cloud droplet formation in global climate models, J. Geophys. Res.-Atmos., 108, 4415, doi:10.1029/2002JD002911, 2003.

Petters, M. D. and Kreidenweis, S. M.: A single parameter representation of hygroscopic growth and cloud condensation nucleus activity, Atmos. Chem. Phys., 7, 1961–1971, doi:10.5194/acp-7-1961-2007, 2007.

Pierce, J. R. and Adams, P. J.: Uncertainty in global CCN concentrations from uncertain aerosol nucleation and primary emission rates, Atmos. Chem. Phys., 9, 1339–1356, doi:10.5194/acp-9-1339-2009, 2009.

Renner, E. and Wolke, R.: Modelling the formation and atmospheric transport of secondary inorganic aerosols with special attention to regions with high ammonia emissions, Atmos. Environ., 44, 1904–1912, 2010.

Rissler, J., Swietlicki, E., Zhou, J., Roberts, G., Andreae, M. O., Gatti, L. V., and Artaxo, P.: Physical properties of the submicrometer aerosol over the Amazon rain forest during the wet-to-dry season transition – comparison of modeled and measured CCN concentrations, Atmos. Chem. Phys., 4, 2119–2143, doi:10.5194/acp-4-2119-2004, 2004.

Segal, Y. and Khain, A.: Dependence of droplet concentration on aerosol conditions in different cloud types: Application to droplet concentration parameterization of aerosol conditions, J. Geophys. Res.-Atmos., 111, D15204, doi:10.1029/2005JD006561, 2006.

Shipway, B. and Abel, S.: Analytical estimation of cloud droplet nucleation based on an underlying aerosol population, Atmos. Res., 96, 344–355, 2010.

Spindler, G., Grüner, A., Müller, K., Schlimper, S., and Herrmann, H.: Long-term size-segregated particle (PM_{10}, $PM_{2.5}$, PM_1) characterization study at Melpitz–influence of air mass inflow, weather conditions and season, J. Atmos. Chem., 70, 165–195, 2013.

Sullivan, R. C., Moore, M. J. K., Petters, M. D., Kreidenweis, S. M., Roberts, G. C., and Prather, K. A.: Effect of chemical mixing state on the hygroscopicity and cloud nucleation properties of calcium mineral dust particles, Atmos. Chem. Phys., 9, 3303–3316, doi:10.5194/acp-9-3303-2009, 2009.

Twomey, S.: The nuclei of natural cloud formation part II: The supersaturation in natural clouds and the variation of cloud droplet concentration, Geofisica pura e applicata, 43, 243–249, 1959.

Wang, J., Cubison, M. J., Aiken, A. C., Jimenez, J. L., and Collins, D. R.: The importance of aerosol mixing state and size-resolved composition on CCN concentration and the variation of the importance with atmospheric aging of aerosols, Atmos. Chem. Phys., 10, 7267–7283, doi:10.5194/acp-10-7267-2010, 2010.

Wang, M. and Penner, J.: Aerosol indirect forcing in a global model with particle nucleation, Atmospheric Chemistry and Physics, 9, 239–260, 2009.

Weisenstein, D. K., Penner, J. E., Herzog, M., and Liu, X.: Global 2-D intercomparison of sectional and modal aerosol modules, Atmos. Chem. Phys., 7, 2339–2355, doi:10.5194/acp-7-2339-2007, 2007.

Wolke, R., Schröder, W., Schrödner, R., and Renner, E.: Influence of grid resolution and meteorological forcing on simulated European air quality: a sensitivity study with the modeling system COSMO–MUSCAT, Atmos. Environ., 53, 110–130, 2012.

Zhao, D. F., Buchholz, A., Kortner, B., Schlag, P., Rubach, F., Fuchs, H., Kiendler-Scharr, A., Tillmann, R., Wahner, A., Watne, Å. K., Hallquist, M., Flores, J. M., Rudich, Y., Kristensen, K., Hansen, A. M. K., Glasius, M., Kourtchev, I., Kalberer, M., and Mentel, Th. F.: Cloud condensation nuclei activity, droplet growth kinetics, and hygroscopicity of biogenic and anthropogenic secondary organic aerosol (SOA), Atmos. Chem. Phys., 16, 1105–1121, doi:10.5194/acp-16-1105-2016, 2016.